Neoplasia • Vol. 9, No. 2, February 2007, pp. 128–135 128

www.neoplasia.com

Visualizing the Acute Effects of Vascular-Targeted Therapy *In Vivo* Using Intravital Microscopy and Magnetic Resonance Imaging: Correlation with Endothelial Apoptosis, Cytokine Induction, and Treatment Outcome[1]

Mukund Seshadri[*,†], *Joseph A. Spernyak*[*], *Patricia G. Maier*[†], *Richard T. Cheney*[‡], *Richard Mazurchuk*[*] *and David A. Bellnier*[†]

*Preclinical Imaging Resources, Department of Cancer Biology, Roswell Park Cancer Institute, Buffalo, NY, USA; †Photodynamic Therapy Center, Department of Cell Stress Biology, Roswell Park Cancer Institute, Buffalo, NY, USA; ‡Department of Pathology and Laboratory Medicine, Roswell Park Cancer Institute, Buffalo, NY, USA

Abstract

The acute effects of the vascular-disrupting agent 5,6-dimethylxanthenone-4-acetic acid (DMXAA) were investigated *in vivo* using intravital microscopy (IVM) and magnetic resonance imaging (MRI). Changes in vascular permeability and blood flow of syngeneic CT-26 murine colon adenocarcinomas were assessed at 4 and 24 hours after DMXAA treatment (30 mg/kg, i.p.) and correlated with induction of tumor necrosis factor-α (TNF-α), endothelial damage [CD31/terminal deoxynucleotidyl transferase (TdT)], and treatment outcome. Intravital imaging revealed a marked increase in vascular permeability 4 hours after treatment, consistent with increases in intratumoral mRNA and protein levels of TNF-α. Parallel contrast-enhanced MRI studies showed a ~ 4-fold increase in longitudinal relaxation rates (ΔR_1), indicative of increased contrast agent accumulation within the tumor. Dual-immunostained tumor sections (CD31/TdT) revealed evidence of endothelial apoptosis at this time point. Twenty-four hours after treatment, extensive hemorrhage and complete disruption of vascular architecture were observed with IVM, along with a significant reduction in ΔR_1 and virtual absence of CD31 immunostaining. DMXAA-induced tumor vascular damage resulted in significant long-term (60-day) cures compared to untreated controls. Multimodality imaging approaches are useful in visualizing the effects of antivascular therapy *in vivo*. Such approaches allow cross validation and correlation of findings with underlying molecular changes contributing to treatment outcome.

Neoplasia (2007) **9,** 128–135

Keywords: Vascular-disrupting agents, DMXAA, multimodality imaging, tumor vasculature, tumor necrosis factor-α.

Introduction

The growth and development of most solid tumors beyond a few millimeters are contingent on the existence of a functioning vascular network [1]. The vascular architecture of tumors is characterized by immature blood vessels with complex branching patterns and irregular geometries that contribute to spatial and temporal variations in blood flow within the tumor [2]. Tumor-associated endothelial cells are abnormally shaped, with loose intercellular connections and focal openings that result in enhanced permeability, compared to normal tissues [3]. These characteristics contribute to metastatic spread and genetic instabilities within the growing tumor that often have a detrimental effect on therapy [4,5]. However, structural and functional differences between normal and tumor vessels have also allowed the development of targeted therapeutics that selectively destroys the tumor vasculature [6]. These vascular-disrupting agents (VDAs) target the endothelial cells of tumors [7] and are, therefore, not associated with multidrug resistance—a characteristic associated with poor clinical prognosis with chemotherapy.

The VDA 5,6-dimethylxanthenone-4-acetic acid (DMXAA) is a small molecule cytokine inducer that is currently undergoing phase II clinical evaluation[2] in the United States in combination with chemotherapeutic agents such as docetaxel [7]. Because VDAs such as DMXAA differ from traditional anticancer cytotoxics in their mechanism of action, they do not always result in significant changes in tumor size [7,8]. Therefore, the present clinical paradigm of monitoring tumor shrinkage may not be a sensitive-enough measure of the true efficacy of these agents.

Abbreviations: VDA, vascular-disrupting agent; DMXAA, 5,6-dimethylxanthenone-4-acetic acid; TNF-α, tumor necrosis factor-α; MRI, magnetic resonance imaging; IVM, intravital microscopy; PECAM, pan endothelial cell adhesion molecule (CD31); TdT, terminal deoxynucleotidyl transferase

Address all correspondence to: David A. Bellnier, Photodynamic Therapy Center, Department of Cell Stress Biology, Roswell Park Cancer Institute, Elm and Carlton Streets, Buffalo, NY 14263. E-mail: david.bellnier@roswellpark.org

[1]This research was supported by National Institutes of Health grants R01CA89656 (D. A. Bellnier) and PO1CA55791 (A. R. Oseroff) and used core facilities at Roswell Park Cancer Institute, which was supported, in part, by National Cancer Institute Cancer Center support grant CA16056.

[2]Clinical trials identifier NCT00119275.

Received 20 November 2006; Revised 5 January 2007; Accepted 8 January 2007.

DOI 10.1593/neo.06748

Furthermore, volume change is a nonspecific biomarker that provides little or no information early on during the course of treatment. It is, therefore, essential to identify and develop early biomarkers that serve as reliable predictors of therapeutic outcome. Imaging-based approaches have proven extremely useful in this regard as they provide early tumor-specific information following treatment well before macroscopic changes in tumor volume become evident.

We have previously demonstrated the usefulness of contrast-enhanced magnetic resonance imaging (MRI) in evaluating the response of human tumor xenografts to DMXAA [9]. The ability of MRI to provide whole-body information with high temporal and spatial resolution in a noninvasive manner is particularly beneficial as it allows serial monitoring of tumor response to therapy, both in preclinical model systems and in clinical settings. However, a single imaging methodology or assay may not adequately reflect the entire spectrum of events that contribute to tumor growth or response to therapy [10]. Multimodality functional imaging approaches, however, would allow a more comprehensive evaluation of tumor response to VDAs such as DMXAA. The utilization of such approaches would also provide complementary information that can be cross-validated and correlated with underlying molecular mechanisms that contribute to eventual treatment outcome.

In this study, we used two advanced imaging techniques, intravital microscopy (IVM) and contrast-enhanced MRI, to visualize and quantitate acute changes in the vascular function of CT-26 murine colon adenocarcinomas following the administration of a single dose of DMXAA. To a large extent, the antivascular–antitumor effects of DMXAA are related to the *in situ* production of the cytokine tumor necrosis factor-α (TNF-α) [11]. However, recent studies have shown that DMXAA results in a variety of pharmacodynamic effects ranging from direct effects on the vascular endothelium to macrophage activation and natural killer cell activity [12,13]. Therefore, in addition to IVM and MRI, the antivascular–antitumor activity of DMXAA was assessed by: 1) dual immunohistochemical staining of tumor sections for pan endothelial cell adhesion molecule (PECAM; CD31) and terminal deoxynucleotidyl transferase (TdT) for detecting endothelial apoptosis; 2) measuring intratumoral mRNA and protein levels of TNF-α in control and DMXAA-treated animals using polymerase chain reaction (PCR) and enzyme-linked immunosorbent assay (ELISA), respectively; and 3) monitoring long-term (60-day) tumor growth following treatment.

Materials and Methods

Tumor Model System

All experimental studies were carried out in the CT-26 murine colon adenocarcinoma model [14] implanted in pathogen-free syngeneic BALB/c-AnNCr mice (Jackson Laboratory, Bar Harbor, ME). Animals were housed in microisolator cages in a laminar flow unit within the animal facility at Roswell Park Cancer Institute (Buffalo, NY) and fed food and water *ad libitum*. For all studies except IVM, 8- to 10-week-old female mice were inoculated subcutaneously with 1×10^6 CT-26 tumor cells harvested from exponentially growing cultures and used for experimentation ~ 7 to 8 days after inoculation, when tumors had reached a diameter of 6 to 7 mm. For IVM studies, ~ 5×10^5 tumor cells were injected within dorsal skinfold window preparations, and studies were carried out 10 to 12 days postimplantation. All studies were performed in accordance with Institutional Animal Care and Use Committee–approved protocols.

DMXAA

DMXAA powder was provided by Gordon Rewcastle (University of Auckland, Auckland, New Zealand) and freshly formulated in 5% sodium bicarbonate before intraperitoneal injection at a dose of 30 mg/kg.

IVM

To visualize changes in vascular architecture and function following DMXAA treatment, intravital imaging based on the dorsal skinfold window preparation was used [15,16]. Briefly, 8- to 10-week-old female BALB/c mice ($n = 5$) were anesthetized with a ketamine/xylazine mixture (10:1) at a dose of 1.0 ml/100 mg. Each mouse was shaved from the neck down to the tail with a clipper and then depilated with Nair (Church & Dwight Co., Inc, Princeton, NJ); the skin was disinfected with hexidine and alcohol. The midline of each animal was then marked with a sterile skin marker, and a "C" clamp was sutured onto the skin of the animal. A circular skin flap ~ 10 mm in diameter was then raised on the dorsal skinfold, leaving all vessels on the opposite side of the skinfold intact. A small amount of saline was periodically injected to keep the surface moist. The two frames of the window chamber were then mounted and secured onto the skin with screws and sutures. Topical antibiotic was applied onto the edges of the wound to prevent subsequent dermal infection. Tumor cells (5×10^5) were then injected into the fascia within the preparation, and the chamber was filled with saline. A glass cover slip was placed over the window preparation, and a retaining ring was applied with pliers on top of the cover slip. Following recovery, mice were transferred onto laminar flow barrier cages containing food and water and placed in a humidified temperature-controlled incubator (32°C). Tumor growth within the window chambers was monitored every 24 hours, and experiments were carried out ~ 10 to 12 days postimplantation, during which tumors grew to ~ 3 to 4 mm, with a well-vascularized network visible within the window chambers. Bright field images were digitally acquired using a surgical microscope with a mounted color camera (Endure Medical, Inc., Cumming, GA) before treatment and 4 and 24 hours after DMXAA administration.

Contrast-Enhanced MRI

All studies were performed using a 4.7-T/33-cm horizontal bore MR scanner (GE NMR Instruments, Fremont, CA) incorporating AVANCE digital electronics (Bruker Medical, Billerica, MA), a removable gradient coil insert (G060; Bruker Medical) generating a maximum field strength of 950 mT/m, and a custom-designed radiofrequency transreceiver coil.

Tumor-bearing mice (n = 7) were anesthetized using 4% isoflurane (Abbott Laboratories, Chicago, IL), secured in a mouse coil chamber, and positioned on the scanner. Anesthesia was maintained at 1% to 2% during imaging, and a circulating water bath maintained at 37°C was used to keep the animals warm inside the magnet. Preliminary noncontrast-enhanced images were acquired before the administration of the contrast agent to obtain regional T_1 measurements. The macromolecular MR contrast agent MacroGd (PharmaIn, Buffalo Grove, IL) was administered manually through tail vein injection at a dose of 0.1 mmol/kg Gd. The agent is a long-circulating gadolinium-containing macromolecule that consists of a monomethoxy ether of polyethylene glycol attached to poly-L-lysine–Gd-DTPA [17,18]. Following administration of the contrast agent, a second set of scans was acquired, and longitudinal relaxation rates (R_1) were calculated using a saturation recovery fast spin-echo sequence with the following: effective time of echo period (TE_{eff}) = 10 milliseconds; repetition time (T_R) = 250 to 6000 milliseconds; field of view (FOV) = 32 × 32 mm; slice thickness = 1 mm; matrix size = 128 × 96; number of averages = 3. In addition, whole-body magnetic resonance angiography (MRA) was performed using a 3D spoiled gradient recalled echo scan (matrix size = 192 × 128 × 128; FOV = 48 × 32 × 32 mm; T_E = 3 milliseconds; T_R = 15 milliseconds; flip angle = 25°). Following pretreatment acquisitions, animals were divided into treatment (n = 4) and control groups (n = 3), and DMXAA (30 mg/kg, i.p.) was administered to the mice in the treatment group. The animals were imaged 4 and 24 hours after treatment, and the change in longitudinal relaxation rates (ΔR_1) was calculated and analyzed for statistically significant differences between the control and treatment groups.

Image processing and analysis were carried out using commercially available software (Analyze PC, Version 5.00; Biomedical Imaging Resource, Mayo Clinic, Rochester, MN). Regions of interest (ROI) of tumors, kidneys, and muscle tissues were manually drawn on the images and object maps of the ROI constructed. The longitudinal relaxation rate ($R_1 = 1/T_1$) for each ROI was computed using MATLAB (Version 7.0; Math Works, Inc., Natick, MA), and source codes were developed by RPCI Preclinical Imaging Resource (Buffalo, NY). To calculate DMXAA-induced changes in vascular function, ΔR_1 was calculated by subtracting postcontrast R_1 values calculated immediately after contrast agent administration from those obtained 4 and 24 hours after contrast agent administration in both control and DMXAA-treated tumors.

Cytokine Measurements

Determination of mRNA and protein levels of TNF-α in CT-26 tumors was performed using reverse transcription (RT) PCR and ELISA, respectively. At different times after DMXAA treatment, tumors were harvested and frozen for processing. Total RNA was extracted from tumors using RNA STAT-60 (Tel-Test, Inc., Friendswood, TX). First-strand synthesis was performed using a first-strand cDNA synthesis kit (K1612; Fermentas, Inc., Hanover, MD) with 2 μg of total RNA. PCR was performed using Platium *Taq* DNA polymerase (InVitrogen Corporation, Carlsbad, CA) for 35 cycles. PCR products were then electrophoresed in 2% agarose in the presence of ethidium bromide. For determination of protein concentrations, tumor tissues were homogenized in cell lysis buffer [CellLytic MT and Protease Inhibitor cocktail; Sigma, St. Louis, MO (400:1)]. Supernatants were isolated, and samples containing 40 μg of protein, as determined by Bio-Rad protein assay (Bio-Rad Laboratories, Hercules, CA), were analyzed for TNF-α expression using an ELISA kit (Quantikine; R&D Systems, Minneapolis, MN) specific for the cytokine. The assays were performed in duplicate on samples isolated from three to four mice for each time point.

Immunohistochemical Analyses

At different times after DMXAA treatment, tumors were harvested and immediately placed in Tris-buffered zinc fixative [0.1 M Tris–HCl buffer (pH 7.4) containing 3.2 mM calcium acetate, 22.8 mM zinc acetate, and 36.7 mM zinc chloride] for 18 hours. The samples were then transferred to 70% ethanol, dehydrated, and embedded in paraffin. After conventional deparaffinization and endogenous peroxidase quenching, 5-μm-thick sections were stained for the PECAM CD31, as described previously [9]. Slides were counterstained with Harris hematoxylin (Poly Scientific, Bayshore, NY). TdT-mediated nick end labeling was used to detect apoptosis in tumor sections using the Apoptag plus Peroxidase *in situ* detection kit (Chemicon International, Inc., Temecula, CA).

Assessment of Tumor Response

Following treatment, the dimensions of subcutaneous tumors were measured with calipers every 1 to 3 days, and tumor volumes were calculated using the formula: $V = 0.52 (L \times W^2)$, where L is the longest axis of the tumor and W is perpendicular to the long axis. Animals were monitored until tumors had reached a volume of 400 mm^3, at which time they were humanely sacrificed. Regrowing tumors reached the 400-mm^3 volume typically within 8 to 10 days. Animals were considered cured if they remained tumor-free for at least 60 days after treatment. The median time to reach 400 mm^3, along with 95% confidence intervals, was estimated for control and DMXAA-treated tumors using the method of Kaplan and Meier [19].

Statistical Analysis

All measured values are reported as the mean ± standard error of the mean. Five animals (control group, two; treatment group, three) were used for IVM studies. For immunohistochemistry and cytokine measurements, at least three mice each were used for the control and treatment groups. Seven animals (control group, three; treatment group, four) were used for MRI. Sixteen animals (control group, 10; treatment group, 6) were used for tumor response studies. Two-tailed *t*-test was used for comparing individual treatment groups with controls. P = .05 was considered statistically significant. The survival curves of untreated control and DMXAA-treated animals were analyzed using log-rank test to test the null hypothesis that the curves were identical. All statistical

calculations and analyses were performed using Graph Pad Prism (Version 4.00; San Diego, CA).

Results

Before imaging the antivascular effects of DMXAA *in vivo*, intravital imaging was performed to observe differences in vascular architecture between tumor and normal tissues. As shown in Figure 1, the skin of a nontumorous BALB/c mouse exhibited a highly organized vascular network with well-defined branching patterns (*control*). To observe changes in vessel geometry during the early stages of tumor growth, serial intravital images were acquired at different times after the injection of CT-26 tumors (Figure 1). By day 4 after implantation of tumor cells in the window chambers, changes in the geometry of host vessels were visible. The vessels appeared dilated in several areas (*yellow arrows*), with some having a high degree of tortuosity compared to day 1. These changes became more obvious on day 6, after implantation with significant vasodilation and increased tortuosity seen within the window chambers (*arrows*). In comparison, the vessels of nontumorous mice did not show such changes in vessel size or tortuosity, highlighting the fact that these changes were tumor-specific and associated with the induction of angiogenesis [16]. On completion of baseline image acquisitions, mice were injected with DMXAA (30 mg/kg, i.p.), and images were acquired 4 and 24 hours after treatment ($n = 3$). As shown in Figure 2, 4 hours after DMXAA treatment, significant vascular leakage was seen within the window chamber, with signs of hemorrhage (*upper panel*). Twenty-four hours after treatment, complete loss of vessel integrity, with severe hemorrhage visible in intravital images, was indicative of DMXAA-induced vascular damage. Inspection of the skin around the window chamber and at a distant site (mouse ear; not shown) revealed no such change in vascular integrity or function, confirming the tumor-selective antivascular activity of DMXAA.

To correlate the intravital findings of tumor response to DMXAA, contrast-enhanced MRI was performed in a parallel study, using a separate cohort of animals ($n = 7$). Whole-body MRA was performed to visualize changes in tumor vascular function following DMXAA (Figure 2, *middle panel*). Consistent with intravital findings, the MRA of DMXAA-treated tumors ($n = 4$) revealed a marked increase in vascular permeability at 4 hours, compared to untreated controls ($n = 3$). Change in enhancement following the administration of the macromolecular MR contrast agent was visualized and quantitated by measuring the change in longitudinal relaxation rate ΔR_1 ($1/T_1$) in tumor and kidney tissues. Kidneys were used as a surrogate measure of contrast agent concentration in the blood. The calculated temporal change in ΔR_1 (tumor/blood) showed a ~ 7-fold increase ($P < .01$) in DMXAA-treated animals (0.708 ± 0.109) compared to untreated controls (0.129 ± 0.05) at this time point (Figure 3). Subsequently, 24 hours after treatment, whereas ΔR_1 values continued to increase in untreated control tumors, mice treated with DMXAA showed a decrease close to baseline levels reflective of DMXAA-induced reduction in vascular perfusion.

Immunohistochemical staining of CT-26 tumor sections for the PECAM along with TdT (CD31/TdT) was performed to

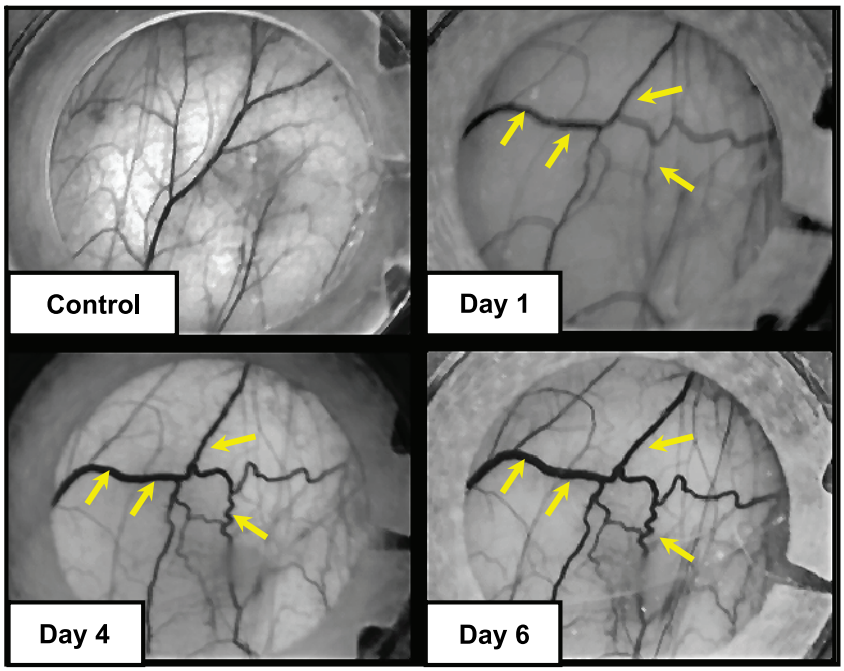

Figure 1. *Intravital microscopic images of normal and tumor-associated vasculature in a BALB/c mouse dorsal skin window chamber. Representative images of normal host cutaneous vasculature (control) and vasculature associated with a growing CT-26 tumor within dorsal skinfold window chambers implanted in BALB/c mice. Serial intravital images were acquired following the injection of CT-26 tumor cells to monitor changes in vessel geometry and architecture with tumor growth. Arrows indicate corresponding areas in the images acquired at different times (days 1, 4, and 6) after tumor implantation that showed significant host vessel dilation and increased tortuosity.*

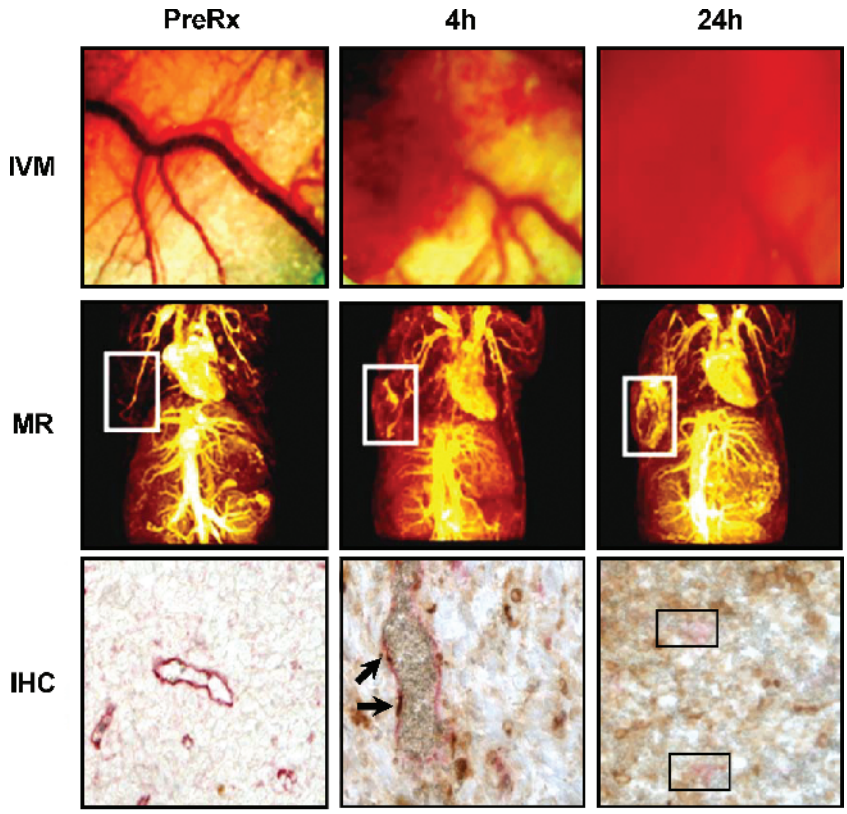

Figure 2. *IVM, contrast-enhanced MRI, and immunohistochemical assessment of CT-26 tumor response to DMXAA. Intravital (upper panel) and contrast-enhanced MR (middle panel) images of CT-26 colon adenocarcinomas acquired before treatment (preRx), 4 hours after treatment with DMXAA (4 h), and 24 hours after treatment with DMXAA (24 h). Imaging-based changes in vascular function correlated with immunohistochemical analysis (CD31/TdT) of tumor sections (lower panel). Four hours after treatment, endothelial apoptosis (arrows) was visible in DMXAA-treated tumors. Ghost outlines of vessels were seen at 24 hours after treatment (rectangles). Representative images of individual mice from each methodology have been shown.*

correlate with changes in image-based parameters of vascular function (Figure 2, *bottom panel*). Tumor sections obtained from untreated control mice showed well-defined clusters of endothelial cells with crisp CD31 staining (Figure 2, *left*). Strong TdT reactivity (*arrows*) was seen in $CD31^+$ blood vessels in CT-26 tumor sections 4 hours after treatment, indicative of endothelial apoptosis (*center*). Twenty-four hours after treatment, extensive TdT reactivity with virtual absence of identifiable CD31 reactive blood vessels was seen (Figure 2, *lower panel*, *right*). Regions of preexisting vessels could be identified by a faint reddish blush (*rectangles*) in tumor sections at this time point.

One of the major biological intermediates believed to be responsible for the antivascular–antitumor activity of DMXAA is TNF-α [11]. To determine whether changes in vascular permeability corresponded with induction of TNF-α, RT-PCR was performed on tumors at different times following treatment (Figure 4*A*). Untreated control CT-26 tumors did not show any upregulation of mRNA for TNF-α. In comparison, increased mRNA levels were detected in DMXAA-treated tumors between 1 and 2 hours after treatment. To further quantify intratumoral cytokine levels in control and DMXAA-treated tumors, ELISA was performed on tumor tissue extracts at 1, 2, and 4 hours after treatment (Figure 4*B*). No significant change ($P > .5$) in TNF-α levels was seen in DMXAA-treated tumors 1 hour after treatment (6.50 ± 0.866) compared to untreated controls (8.25 ± 0.75). Consistent with RT-PCR data, a marked increase (~ 20-fold) in intratumoral concentrations of TNF-α was detected at 2 hours after treatment (285.8 ± 37.76; $P < .001$ *vs* control). TNF-α levels measured in tumors 4 hours after DMXAA treatment showed a further increase (443.5 ± 48.52; $P = .0001$) compared to untreated controls. The difference in TNF-α levels between the 2-hour and the 4-hour time points was also statistically significant ($P < .05$).

Finally, to determine the effects of DMXAA-based antivascular therapy on long-term treatment outcome, tumor-bearing mice were injected with DMXAA (30 mg/kg) and monitored for a period of 60 days following treatment for tumor regrowth. Survival curves based on the Kaplan-Meier method were generated for untreated controls and DMXAA-treated animals. As seen in Figure 5, DMXAA resulted in significant tumor control, with ~ 80% of the mice remaining tumor-free at 60 days ($P < .001$).

Discussion

The essential role of the vasculature in malignant progression, combined with the differential characteristics of tumor and normal vessels, has led to the development of therapeutics that either disrupt existing tumor vessels (VDAs) or inhibit new vessel formation (antiangiogenics) [1,8]. These

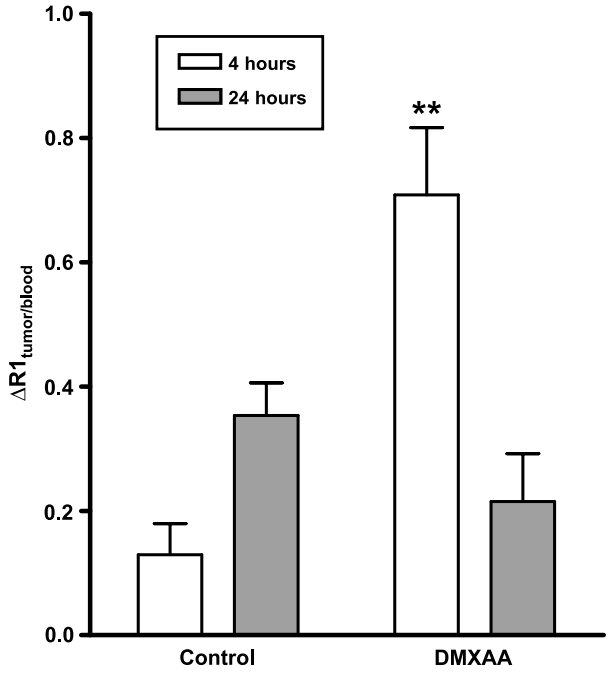

Figure 3. *Temporal change in the longitudinal MR relaxation rate (ΔR_1 tumor/blood) of control and DMXAA-treated CT-26 tumors implanted in BALB/c mice. Graph shows the change in T_1 relaxation rates (ΔR_1) over time of untreated control tumors (squares) and tumors treated with 30 mg/kg DMXAA following administration of the macromolecular contrast agent. Significant differences in ΔR_1 values (**P < .01; two-tailed t-test) were seen 4 hours after DMXAA treatment (n = 3) compared to untreated controls (n = 3).*

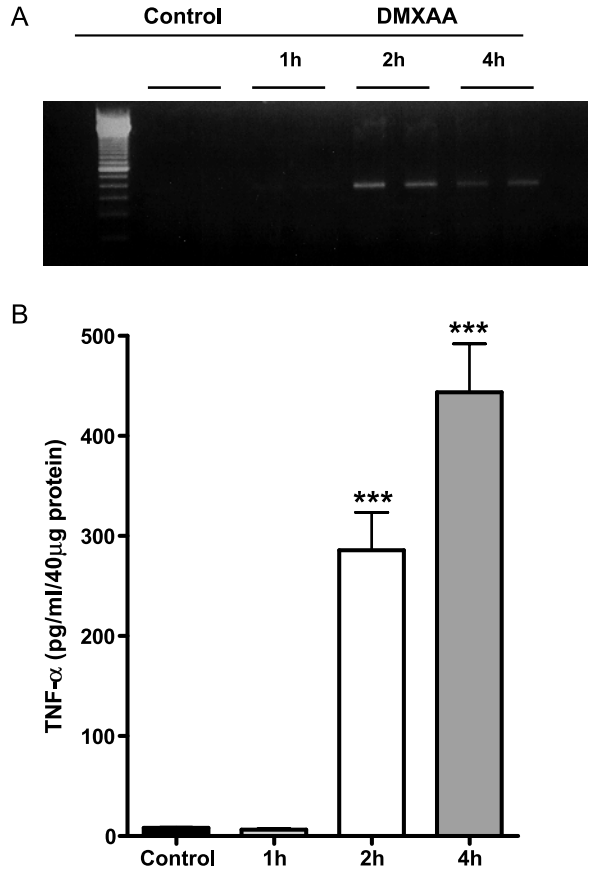

Figure 4. *Induction of TNF-α at different times after DMXAA treatment. BALB/c mice bearing subcutaneous CT-26 tumors were injected with DMXAA and, at different times after treatment, tumors were excised for the determination of mRNA (A) and protein levels of TNF-α (B) using PCR and ELISA, respectively. Statistical analyses (two-tailed t-test) revealed significant differences between control and treatment groups at 2 and 4 hours after treatment (***P < .001). At least three to four mice were used for each time point.*

biological therapies that selectively target tumors differ fundamentally in their mechanism(s) of action from conventional cancer chemotherapies and do not always result in tumor shrinkage following treatment [7,8]. This is particularly important as anatomical imaging-based approaches that have traditionally been used to assess tumor response to chemotherapy or radiation therapy rely on volumetric change and may not be beneficial in the evaluation of vascular-targeted therapies. Furthermore, it is widely recognized that molecular alterations within the tumor occur much before macroscopic changes in gross tumor volume can be detected. It is, therefore, essential to use functional imaging techniques that provide early quantitative end points reflective of underlying biological change.

The purpose of this study was to assess the antivascular effects of the VDA DMXAA *in vivo* using a multimodality imaging approach and to correlate imaging-based changes in vascular function with underlying molecular changes that contributed to its antitumor effect. Using two advanced imaging techniques, IVM and contrast-enhanced MRI, acute vascular changes following DMXAA administration were evaluated in a murine carcinoma model. Alterations in tumor vascular permeability and perfusion following treatment correlated with endothelial apoptosis, intratumoral levels of TNF-α, and long-term tumor response.

Intravital imaging based on the dorsal skinfold window chamber technique is an extremely useful method that allows visualization of tumor vessels in real time at high resolution [16]. The ability of IVM to allow a serial assessment of tumors

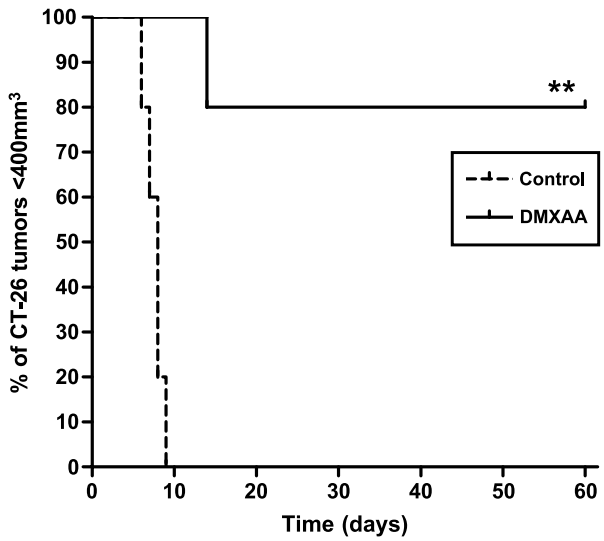

Figure 5. *Long-term treatment outcome following antivascular therapy. BALB/c mice bearing subcutaneous CT-26 tumors were injected with 30 mg/kg DMXAA, and tumor growth was monitored for 60 days after treatment. Kaplan-Meier survival curves of untreated controls (n = 10) and DMXAA-treated animals (n = 6). A significant difference in survival was seen between control and treatment groups (**P < .01; log-rank test).*

is particularly useful in studying molecular events associated with angiogenesis and the response of tumors to antiangiogenic or antivascular therapies [16,20]. In the present study, vascularization of CT-26 tumors within the dorsal skinfold window chamber was clearly visualized, with changes in vascular architecture visible as early as 2 days after implantation (Figure 1). Intravital imaging showed evidence of altered permeability 4 hours after DMXAA administration. This is in agreement with a previous study by Zhao et al. [21], in which, using Evans blue extravasation, it was demonstrated that the major mechanism of action of DMXAA was increase in tumor vascular permeability. Twenty-four hours after treatment, complete destruction of tumor vascular architecture was seen with IVM, consistent with previous preclinical reports of reduction in vascular perfusion and onset of necrosis at this time point [21,22]. Intravital imaging offers the ability to directly visualize angiogenesis and tumor vascular response to treatment in a live animal; however, due to its invasive nature and the requirement of a specialized surgical preparation of tissues, it cannot be readily translated into the clinical setting. To validate IVM findings, parallel studies were carried out using MRI.

Contrast-enhanced MRI is a noninvasive imaging technique that provides functional images of the tumor vasculature in animal models and is routinely used in humans [23]. Although resolution of individual tumor vessels is difficult with MRI, the technique offers excellent tissue contrast and provides whole-body renderings that allow the simultaneous evaluation of tumor and normal tissues. Several preclinical and clinical studies have used dynamic contrast-enhanced (DCE) MRI to assess the response of tumors to VDAs such as DMXAA and CA4P, with limited success [22,24]. A majority of these DCE-MRI studies have been performed using small molecule MR contrast agents, typically Gd-DTPA, to estimate parameters of tumor vascular permeability (K^{trans}) and blood flow (area under the curve) following treatment. However, reduction in these parameters has only been inconsistently observed in preclinical studies, particularly with DMXAA [24,25]. Even in the phase I clinical trial of DMXAA, DCE-MRI parameters did not reveal a dependable dose response in patients, questioning the true clinical utility of the technique [25]. In comparison, several studies have reported the usefulness of macromolecular MR contrast agents for measuring changes in the permeability and perfusion of tumors in response to inhibitors of angiogenesis [18,26]. In this study, we used one such macromolecular contrast agent that exhibits a longer intravascular distribution compared to Gd-DTPA [17]. The long half-life and low first-pass elimination of the agent allowed the monitoring of changes in vascular permeability/perfusion with a single injection. The agent has been shown to be nonimmunogenic, capable of producing superior quality images with high contrast-to-noise ratio, and useful in the assessment of antiangiogenic therapies [17,18].

The selective destruction of the tumor vasculature leading to the secondary ischemic necrosis of tumor cells is the fundamental basis of the antitumor activity of DMXAA [13]. The development of DMXAA was based on the selective induction of TNF-α *in situ* [11]. TNF-α is a pleiotropic cytokine that is produced mainly by activated cells of monocyte/macrophage lineage [27]. TNF-α has been shown to cause the necrosis of tumors in experimental animals, primarily through toxic effects on the tumor vasculature [28]. The antivascular effects of DMXAA are, therefore, believed to be, at least in part, related to the effects of TNF-α [11]. The induction of TNF-α following DMXAA treatment has been studied extensively in murine tumors and human tumor xenografts [11,29]. In our study, intratumoral measurements of TNF-α showed a strong correlation to observed changes in vascular permeability (Figure 4). This is not surprising as the effects of TNF-α on the vascular endothelium have been previously shown to include changes in the shape and motility of endothelial cells, upregulation of adhesion molecules such as E-selectin, and the recruitment and activation of leukocytes [28,30,31]. These, in turn, result in the initiation of vascular injury, loss of vascular tone, and increase in endothelial permeability.

Although the major mechanism of action of DMXAA is believed to be the induction of TNF-α *in situ*, recent studies have shown evidence of direct drug toxicity to the vascular endothelium [12]. Reductions in tumor blood flow have been observed early on after the administration of DMXAA, much before changes in plasma or tumor TNF-α levels can be measured [12]. This has been attributed to direct drug-induced endothelial damage that results in a cascade of events ranging from exposure of basement membrane to platelet activation to serotonin release and changes in vascular permeability [12,13]. In a previous study by Ching et al. [12], induction of endothelial cell apoptosis has been observed within 30 minutes of the administration of 25 mg/kg DMXAA to Colon-38 tumor-bearing mice without any detectable apoptosis of tumor cells. In the same study, endothelial cell apoptosis was also reported to have been observed in a breast carcinoma biopsy from a patient in the phase I trial of DMXAA. In the murine carcinoma model used in our study, a similar evidence of endothelial apoptosis was seen 30 minutes after DMXAA (data not shown). In our study, tumor sections dual-stained for CD31/TdT showed clear evidence of endothelial apoptosis at 4 hours (Figure 2), indicating that the increased vascular permeability seen at this time point is a cumulative effect of both direct drug effects on the endothelium and indirect effects mediated by cytokine induction. Twenty-four hours after DMXAA treatment, CT-26 tumor sections showed a virtual absence of CD31 reactivity indicative of significant vascular damage, further highlighting the relationship between endothelial damage and reduction in vascular perfusion. Taken together, the results of our study show that DMXAA resulted in an early dramatic increase in vascular permeability that is visible after a few hours of treatment, consistent with endothelial damage and increased cytokine induction. These changes subsequently led to complete disruption of vascular architecture, reduction in blood flow, and a high percentage of tumor cures.

In conclusion, multimodality imaging of the vasculature with a high degree of correlation is feasible *in vivo* and is a useful tool in the assessment of antivascular and antiangiogenic therapies. Although a number of functional imaging techniques are currently being studied or are in progress,

there has been little validation of imaging methodologies with accepted molecular surrogates of disease process or treatment outcome. In this report, we have demonstrated the usefulness of a multimodality approach using two complementary advanced imaging techniques, IVM and MRI, to understand and characterize response to antivascular therapy in an experimental tumor model. Although quantitative estimates of changes in vessel geometry (lumen size or diameter) were not performed, to the best of our knowledge, this is the first study wherein direct visualization of the response of individual tumor vessels to DMXAA using IVM has been reported. Studies aiming to visualize and quantitate functional changes in tumor vessels (vascular resistance and red blood cell velocity) in response to DMXAA treatment are currently being planned in our laboratory. One limitation of our study was the use of separate cohorts of animals for IVM and MRI studies. Although the window chambers used in the study are nonmagnetic, preliminary MRI studies carried out on animals implanted with these titanium-based window chambers revealed significant artifacts at the tissue–chamber interface, which prevented the accurate visualization of corresponding areas on the same group of animals with both techniques. We are currently exploring the potential utility of an MR-compatible window chamber that allows the simultaneous assessment of tumor vascular response to therapy using MRI and IVM within the same animal. Preliminary studies have revealed encouraging results with good correlation between the two techniques [32]. Studies aiming to develop image-based algorithms that will allow coregistration of functional images from multiple imaging techniques are also ongoing in our laboratory. We believe that the successful development of these coregistration algorithms will enable the utilization of complementary imaging techniques to make meaningful comparisons between different results obtained and to provide insights into the mechanism(s) of action of vascular-targeted therapies *in vivo*.

References

[1] Folkman J (1971). Tumor angiogenesis: therapeutic implications. *N Engl J Med* **285**, 1182–1186.

[2] Less JR, Skalak TC, Sevick EM, and Jain RK (1991). Microvascular architecture in a mammary carcinoma: branching patterns and vessel dimensions. *Cancer Res* **51**, 265–273.

[3] Hashizume H, Baluk P, Morikawa S, McLean JW, Thurston G, Roberge S, Jain RK, and McDonald DM (2000). Openings between defective endothelial cells explain tumor vessel leakiness. *Am J Pathol* **156**, 1363–1380.

[4] Boucher Y, Baxter LT, and Jain RK (1990). Interstitial pressure gradients in tissue isolated and subcutaneous tumors: implications for therapy. *Cancer Res* **50**, 4478–4484.

[5] Gillies RJ, Schornack PA, Secomb TW, and Raghunand N (1999). Causes and effects of heterogenous perfusion in tumors. *Neoplasia* **1**, 197–207.

[6] Denekamp J (1982). Endothelial cell proliferation as a novel approach to targeting tumour therapy. *Br J Cancer* **45**, 136–139.

[7] Tozer GM, Kanthou C, and Baguley BC (2005). Disrupting tumour blood vessels. *Nat Rev Cancer* **5**, 423–435.

[8] Kelland LR (2005). Targeting established tumor vasculature: a novel approach to cancer treatment. *Curr Cancer Ther Rev* **1**, 1–9.

[9] Seshadri M, Mazurchuk R, Spernyak JA, Bhattacharya A, Rustum YM, and Bellnier DA (2006). Activity of the vascular disrupting agent 5,6-dimethylxanthenone-4-acetic acid against human head and neck carcinoma xenografts. *Neoplasia* **8**, 534–542.

[10] McDonald DM and Choyke PL (2003). Imaging of angiogenesis: from microscope to clinic. *Nat Med* **9**, 713–725.

[11] Joseph WR, Cao Z, Mountjoy KG, Marshall ES, Baguley BC, and Ching L (1999). Stimulation of tumors to synthesize tumor necrosis factor-alpha *in situ* using 5,6-dimethylxanthenone-4-acetic acid: a novel approach to cancer therapy. *Cancer Res* **59**, 633–638.

[12] Ching L-M, Cao Z, Kieda C, Zwain S, Jameson MB, and Baguley BC (2002). Induction of endothelial cell apoptosis by the antivascular agent 5,6-dimethylxanthenone-4-acetic acid. *Br J Cancer* **86**, 1937–1942.

[13] Baguley BC and Ching L-M (2002). DMXAA: an antivascular agent with multiple host responses. *Int J Radiat Oncol Biol Phys* **54**, 1503–1511.

[14] Brattain MG, Stevens JS, Fine D, Webb M, and Sarrif AM (1980). Establishment of mouse colonic carcinoma cell lines with different metastatic properties. *Cancer Res* **40**, 2142–2146.

[15] Wu NZ, Klitzman B, Dodge R, and Dewhirst MW (1992). Diminished leukocyte endothelium interaction in tumor microvessels. *Cancer Res* **52**, 4265–4268.

[16] Li C, Shan S, Huang Q, Braun R, Lanzen J, Hu K, Lin P, and Dewhirst M (2000). Initial stages of tumor cell–induced angiogenesis: evaluation *via* skin window chambers in rodents. *J Natl Cancer Inst* **92**, 143–147.

[17] Bogdanov AA Jr, Weissleder R, Frank H, Bogdanova AV, Nossiff N, Schaffer B, Tsai E, Papisov M, and Brady TJ (1993). A new macromolecule as a contrast agent for MR angiography: preparation, properties and animal studies. *Radiology* **187**, 701–706.

[18] Lewin M, Bredow S, Sergeyev N, Marecos E, Bogdanov A Jr, and Weissleder R (1999). *In vivo* assessment of vascular endothelial growth factor–induced angiogenesis. *Int J Cancer* **83**, 798–802.

[19] Kaplan EL and Meier P (1958). Nonparametric estimation from incomplete observations. *J Am Stat Assoc* **53**, 457–481.

[20] Lozonschi L, Sunamura M, Kobari M, Egawa S, Ding L, and Matsuno S (1999). Controlling tumor angiogenesis and metastasis of C26 murine colon adenocarcinoma by a new matrix metalloproteinase inhibitor, KB-R7785, in two tumor models. *Cancer Res* **59**, 1252–1258.

[21] Zhao L, Ching LM, Kestell P, Kelland LR, and Baguley BC (2005). Mechanisms of tumor vascular shutdown induced by 5,6-dimethylxanthenone-4-acetic acid (DMXAA): increased tumor vascular permeability. *Int J Cancer* **116**, 322–326.

[22] McPhail LD, McIntyre DJO, Ludwig C, Kestell P, Griffiths JR, Kelland LR, and Robinson SP (2006). Rat tumor response to the vascular disrupting agent 5,6-dimethylxanthenone-4-acetic acid as measured by dynamic contrast-enhanced magnetic resonance imaging, plasma 5-hydroxyindoleacetic acid levels and tumor necrosis. *Neoplasia* **8**, 199–206.

[23] Padhani A (2003). MRI for assessing antivascular cancer treatments. *Br J Radiol* **76**, S60–S80.

[24] Beauregard DA, Pedley RB, Hill SA, and Brindle KM (2002). Differential sensitivity of two adenocarcinoma xenografts to the anti-vascular drugs combretastatin A4 phosphate and 5,6-dimethylxanthenone-4-acetic acid, assessed using MRI and MRS. *NMR Biomed* **15**, 99–105.

[25] Galbraith SM, Rustin GJ, Lodge MA, Taylor NJ, Stirling JJ, Jameson M, Thompson P, Hough D, Gumbrell L, and Padhani AR (2002). Effects of 5,6-dimethylxanthenone-4-acetic acid on human tumor microcirculation assessed by dynamic contrast-enhanced magnetic resonance imaging. *J Clin Oncol* **20**, 3826–3840.

[26] Kim YR, Yudina A, Figueiredo J, Reichardt W, Hu-Lowe D, Petrovsky A, Kang HW, Torres D, Mahmood U, Weissleder R, et al. (2005). Detection of early antiangiogenic effects in human colon adenocarcinoma xenografts: *in vivo* changes of tumor blood volume in response to experimental VEGFR tyrosine kinase inhibitor. *Cancer Res* **65**, 9253–9260.

[27] Van Horssen R, ten Hagen TLM, and Eggermont AMM (2006). TNF-alpha in cancer treatment: molecular insights, antitumor effects, and clinical utility. *Oncologist* **11**, 397–408.

[28] Watanabe N, Niitsu Y, Umeno H, Kuriyama H, Neda H, Yamauchi N, Maeda M, and Urushizaki I (1988). Toxic effect of tumor necrosis factor on tumor vasculature in mice. *Cancer Res* **48**, 2179–2183.

[29] Philpott M, Baguley BC, and Ching L-M (1995). Induction of tumour necrosis factor-alpha by single and repeated doses of the antitumour agent 5,6-dimethylxanthenone-4-acetic acid. *Cancer Chemother Pharmacol* **36**, 143–148.

[30] Rainer GG (1996). Tumor necrosis factor–induced E-selectin expression on vascular endothelial cells. *Crit Care Med* **24**, 1543–1546.

[31] Friedl J, Puhlmann M, Bartlett DL, Libutti SK, Turner EN, Gnant MFX, and Alexander HR (2002). Induction of permeability across endothelial cell monolayers by tumor necrosis factor (TNF) occurs *via* a tissue factor–dependent mechanism: relationship between the procoagulant and permeability effects of TNF. *Blood* **100**, 1334–1339.

[32] Seshadri M, Spernyak J, Bellnier D, and Mazurchuk R (2006). Multimodality imaging of vasculature *in vivo*. *Soc Mol Imaging* (Abstract 335).